Commun. Comput. Chem.
doi: 10.4208/cicc.2013.v1.n2.9

Vol.**1**, No.**2**, pp. 191-203
April 2013

REGULAR ARTICLE

Mechanism of CO_2 Activation by (PNN)Ru(H)(CO) Complex

Xiang Zhang*[1], Shuangshuang Liu

[1]*School of Chemistry and Materials Science, Shanxi Normal University, Linfen, China, P. R. 041004*

Received 23 December 2012; Accepted (in revised version) 5 February 2013

Special Issue: Guo-Zhong He Festschrift

Abstract: The reaction mechanism for CO_2 activation by (PNN)Ru(H)(CO) was comprehensively investigated by means of density functional theory method. The theoretical results indicate that: 1) isomer **1** (with methylene in phosphorus side arm**)** is more stable than **2** (with methylene in amide side arm**)** by 6.45 kcal/mol, and two hydrogen migration steps with barrier heights of 49.95 and 38.24 kcal/mol, respectively, are involved in the tautomerism between **1** and **2**; 2) The direct [1,3]-addition of CO_2 to **1** and **2** affords **4** and **5**, respectively, by forming new C-C and Ru-O bonds. The addition barriers are calculated to be 9.83 and 6.66 kcal/mol, while the decomposition barriers of **4** and **5** are 7.97 and 19.38 kcal/mol, respectively; 3) Reverse [1,3]-additions leading to **6** and **7** are thermodynamically and kinetically unfavorable. The frontier molecular orbital analysis shows that CO_2 [1,3]-addition leading to **4** and **5** is preferred to inverse [1,3]-addition leading to **6** and **7**, respectively.

AMS subject classifications: 65D17, 65D18, 68U05, 68U07

Key words: (PNN)Ru(H)(CO), CO_2, activation, mechanism, pincer ligand, density functional theory

1. Introduction

In the past few decades, cooperative catalysis based on new modes of metal ligand

* Corresponding author. *Email address*: xiangzh2000@hotmail.com (Xiang Zhang) Tel: 86-357-2051192 Fax: 86-357-2051192

cooperation has experienced an explosive progress for their powerful catalytic activity in the asymmetric synthesis. PNN-, PNS- and PNP-type ruthenium pincer complexes have shown substantial catalytic activity in a variety of reactions [1-5]. A series of recent reports by Milstein have demonstrated that pincer-ligated Ru complexes such as (PNN)Ru(H)(CO) (PNN=6-(di-tert-butylphosphinomethylene)-2-(N,N-diethylaminomethyl)-1,6-dihydropyridine) and (PNP)Ru(H)(CO) (PNP=2,6-(di-tert-butylphosphinomethylene) -1,6-dihydropyridine) are highly effective catalysts for the hydrogenation of carbonyl compounds, including esters, amides, and carbamides[6-16].

2012, Milstein and co-workers [17] reported the cooperative [1,3]-addition of CO_2 to the unsaturated PNP-pincer complex [Ru(PNPtBu*)(H)(CO)]. Their experimental results showed that CO_2 [1,3]-addition via forming new C-C and Ru-O bonds was proved to be the most feasible reaction mode, and they demonstrated that dispersion correction is very important in mechanism study by density functional theory.

2012, Sanford and co-workers reported the activation of CO_2 at (PNN)Ru(H)(CO) via C−C coupling with the pincer ligand in conjunction with Ru−O bond formation under mild condition [18]. The discoveries have great practical significance in synthetic chemistry as well as the reutilization of carbon dioxide [19]. Although Sanford and co-workers proposed similar catalytic mechanism as CO_2 activation by PNP-Ru complex [17], the detailed mechanism, especially the information of the rate-determining step of CO_2 activation by PNN-Ru complex, is still unknown.

In this paper, we present the computational investigations into the mechanism of the CO_2 activation reaction by (PNN)Ru(H)(CO) using the density functional theory. The mechanisms of tautomerization between the two isomers of (PNN)Ru(H)(CO), and their [1,3]-addition reaction with CO_2 were fully considered. The essential role of noninnocent pincer ligand in the rate-determining step of CO_2 activation processes was revealed and analyzed in depth.

2. Computational Methods

All geometric optimizations and vibration analysis were performed with the Gaussian03 program package [20]. B3LYP method with combined basis set, 6–311G (d, p) for all nonmetal atoms and Def2-SVP for Ru atom, was employed in all the calculations. Geometries of all the stationary points, including reactants, products, intermediates and transition states, were fully optimized without any constrains. All the minima and transition states were further proved by vibrational analysis to ensure no imaginary mode for minima, and one and only one imagine mode for transition states. Intrinsic reaction coordinate (IRC)

[21] calculations were carried out in both forward and reverse directions, and correction linkage of two minima (x and y) by transition state $\mathbf{TS}_{x/y}$ was confirmed.

For inclusion of solvation effect of C_6H_6 (298 k, 1atm), single point energy calculations were performed with Gaussian09 program package [22], using the integral equation-formalism polarizable continuum model (IEF-PCM) [23-28], Specifically, Truhlar's empirically parameterized version Solvation Model Density (SMD) [29] was used.

The empirical dispersion correction as recommended by Grimme [30, 31] was added to the B3LYP energies, using the stand-alone program (DFTD3) written by Grimme [32].

In this paper, relative free Gibbs energies in C_6H_6 solution are used in discussion. The energy for each species in solution is taken through eq1:

$$G_{sol} = E_{SMD} + (G - E) \quad (1)$$

E_{SMD} is the IEFPCM energy calculated with SMD in benzene and *(G-E)* is the difference between the Gibbs and potential energies, which includes the zero-point, thermal and entropy corrections in gas phase.

3. Results and Discussion

(1) Tautomerization between 1 and 2

At first we consider the tautomerization mechanism between complex **1** and **2**. **Figure 1** predicts the relative energy profile of tautomerization between **1** and **2**. The optimized structures of reactants, products, transition states and intermediates are shown in Figure 2. From **Figure 1**, one can see that **1** is located lower than **2** by 6.45 kcal/mol and there are two pathways for the conversion between **1** and **2**: Pathway A (PW-A) which involves a non-hydride Ru intermediate **3**, and pathway B (PW-B) which involves a dihydride Ru intermediate **3'**.

In PW-A, firstly, hydrogen (H1) transfers from Ru atom to the unsaturated carbon atom of the phosphorus side methylene (C1) to form an intermediate **3** through transition state $\mathbf{TS}_{1/3}$, then hydrogen (H2) at the C atom of the $N(Et)_2$ side arm migrates to Ru atom via transition state $\mathbf{TS}_{2/3}$ to give **2**. From **Figure 2**, it can be seen that the C1-C2 bond distance in **3 (**1.508 Å**)** is 0.123 Å longer than that in **1** (1.385 Å). The C3-C4 bond distance in **2** (1.363) is 0.146 Å shorter than that in **3** (1.509 Å). These structural changes indicate that the hydrogen migration process is concomitant with the breaking of C1=C2 π bond and the formation of C3=C4 double bond. For PW-A, the calculated barriers for the two hydrogen migration steps are 49.95 and 38.24 kcal/mol, respectively, and intermediate **3** is located higher than **1** plus

CO_2 by 9.21 kcal/mol.

PW-B also has two hydrogen migration steps: the first step is hydrogen (H2) migration from the C atom of the $N(Et)_2$ side arm to Ru and affords dihydride Ru intermediate **3′**, and the second step is H1 migration from Ru atom to the C atom of the phosphorus side methylene. The calculated relative energy of **3′, $TS_{1/3'}$** and **$TS_{2/3'}$** are 60.68, 74.05 and 73.61 kcal/mol, respectively. It is obvious that the two hydrogen migration barriers in PW-B are much higher than those in PW-A, so PW-B is less competitive than PW-A.

Based on above theoretical results, tautomerization of **1** to **2** mainly takes place via PW-A. However, due to the high barrier heights in PW-A, the conversion rate of **1** to **2** should be very slow at room temperature.

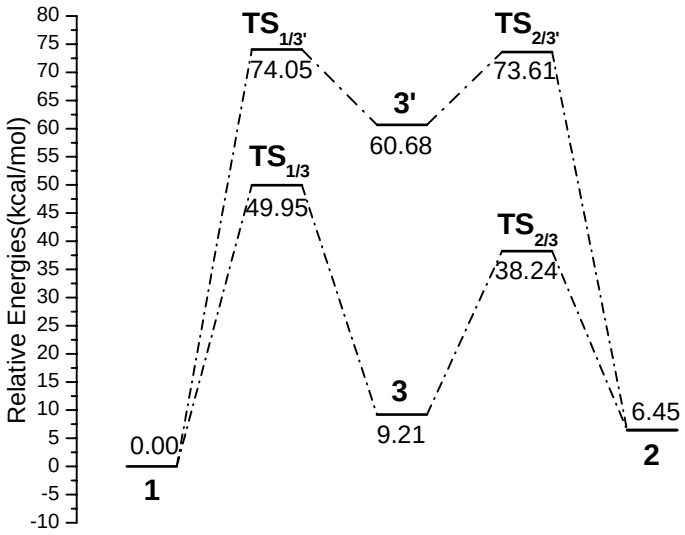

Figure 1: Relative energy profile for the tautomerization between **1** and **2**.

(2) Formation of 4 and 5

Figure 3 depicts the [1,3]-addition mechanism for CO_2 reaction with **1** and **2**, which leads to **4** and **5**, respectively. The reverse [1,3]-addition products, **6** and **7**, are also given in **Figure 3.** First of all, one can notice that **6** and **7** (with relative energies of 34.31 and 21.59 kcal/mol, respectively) are located much higher than **4** and **5**, and are even higher than **$TS_{1/4}$** and **$TS_{2/5}$**. So it is obvious that reverse [1,3]-addition mechanism for CO_2 reaction with **1** and **2** is both thermodynamically and kinetically unfavorable. Therefore, in the following, only the [1,3]-addition mechanism that leading to **4** and **5** is discussed in detail.

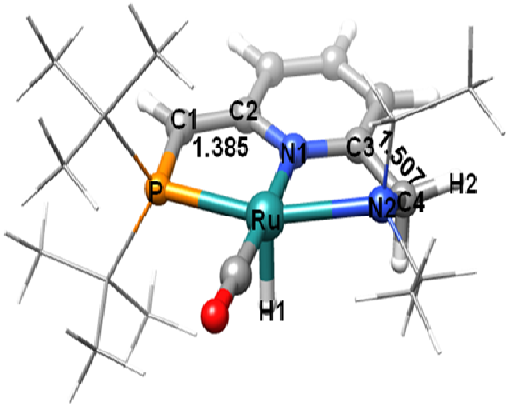

1

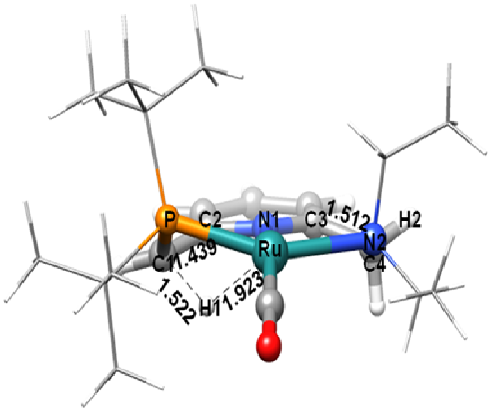

TS1/3

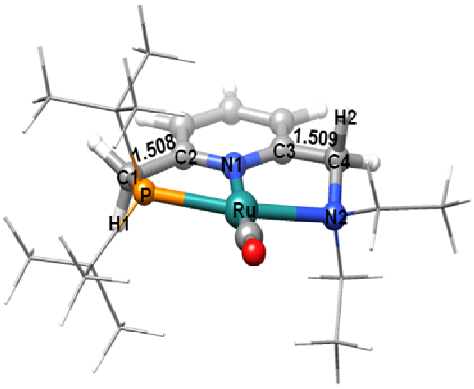

3

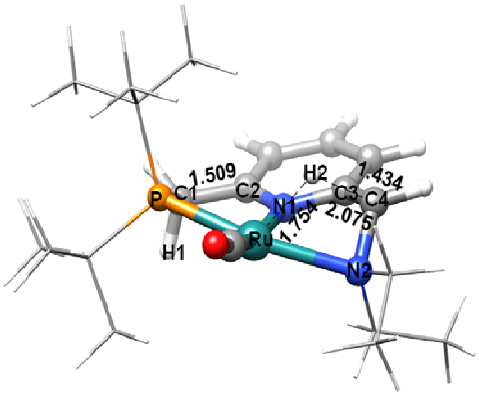

TS2/3

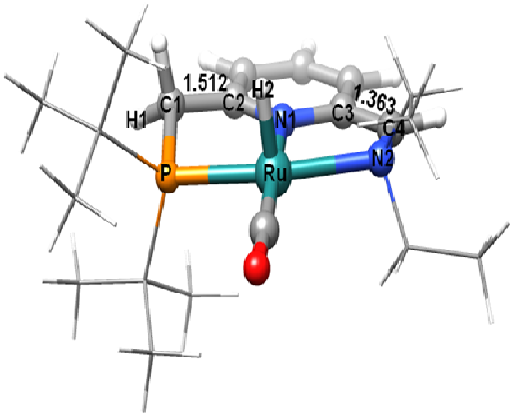

2

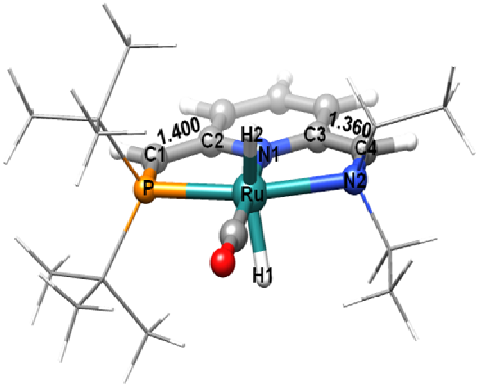

3′

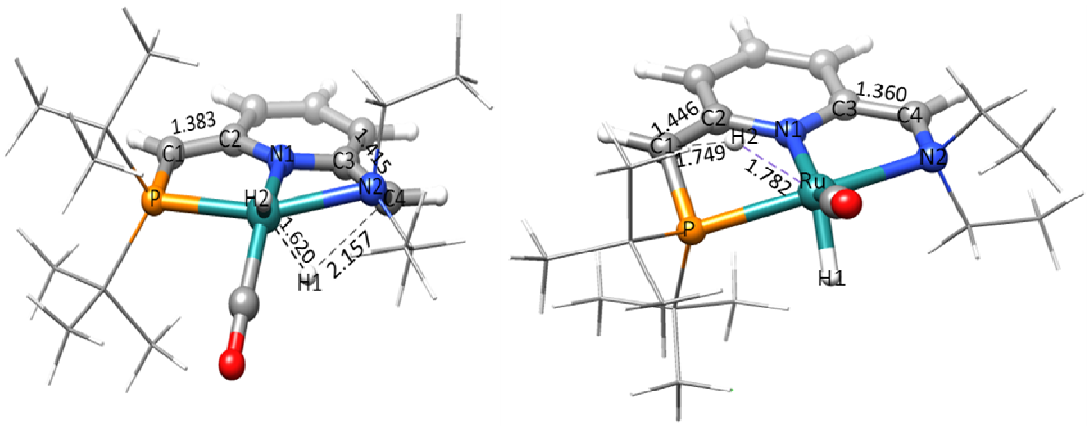

TS$_{1/3'}$ **TS**$_{2/3'}$

Figure 2: Optimized structures of the intermediate (**1**, **2**, **3** and **3′**) and transition states (**TS**$_{1/3}$ and **TS**$_{2/3}$, and **TS**$_{1/3'}$ and **TS**$_{2/3'}$), along with the key bond lengths (Å).

[1,3]-addition reactions of CO_2 with **1** and **2** lead to **4** and **5**, respectively via **TS**$_{1/4}$ and **TS**$_{2/5}$. In this [1,3]-addition process, the electrophilic carbon atom of CO_2 adds to the unsaturated carbon in the phosphorus or amide side arm of the pincer ligand to form a new C-C bond, and simultaneously a Ru-O bond is formed. New C-C bond formation destroys the π interaction between pyridine ring and side arm. As the results, the C1-C2 distance in **4** (1.492 Å) and the C3-C4 distance in **5** (1.502 Å) are significantly elongated compared to those observed in the linking intermediates **1** and **2**, respectively. One can notice that, the C1-C5 and Ru-O1 distances in **4** are longer than the C4-C5 and Ru-O1 distances in **5** by 0.023 Å and 0.042 Å, respectively. These results indicate that the bonding interaction between CO_2 and (PNN)Ru(H)(CO) moieties in **5** are stronger than that in **4**. In **5**, the Ru−N1, Ru−N2, and Ru−P bond lengths are 2.111, 2.262, and 2.304 Å, respectively, which are nearly identical with those of the experimental values [18], 2.090, 2.233, and 2.265 Å, respectively.

[1,3]-addition of CO_2 with **1** gives the intermediate **4** through a transition state **TS**$_{1/4}$ with barrier height 9.83 kcal/mol, and the step is slightly endothermic by 1.85 kcal/mol. CO_2 adds to **2** leading to **5** by crossing the transition state **TS**$_{2/5}$ with 6.66 kcal/mol barrier and is exothermal by 12.72 kcal/mol. Both the activation energies are quite small, therefore the two addition reactions should be very fast. Due to the high conversion barriers between **1** and **2**, only CO_2 addition with **1** leading to **4** is kinetically predominant reaction pathway at room temperature. Meanwhile, the decomposition barriers for **4** and **5** are 7.97 and 19.38 kcal/mol, respectively. So, at room temperature, the C-C bond formation is reversible at **4**, but irreversible at **5** [18]. Since **5** is located lower than **4** by 8.12 kcal/mol, conversion of **4** to **5** via

channel **4→1→2→5** may occur slowly at room temperature, or be accelerated at elevated temperature. These theoretical results are in good agreement with experimental findings [18].

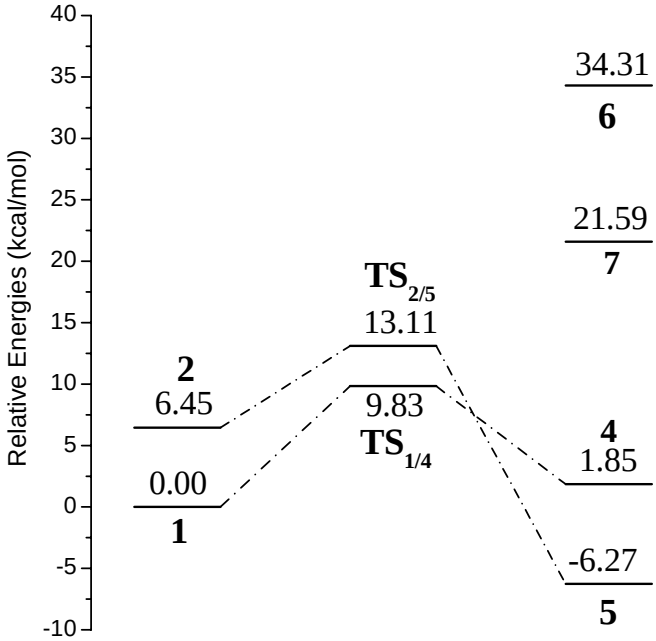

Figure 3: Relative energy profiles for the forming of **4** and **5.**

The calculated barrier heights of CO_2 [1,3]-addition to PNN-Ru complex(9.83 kcal/mol for forming **4** and 13.11 kcal/mol for forming **5**), are higher than the calculated barrier height of CO_2 [1,3]-addition to PNP-Ru complex (8.10 kcal/mol in THF and 7.5 kcal/mol in C_6H_6, [17]). It is noteworthy that, in this study, dispersion correction was only included in relative energies but not in geometry optimizations (which is not allowed for B3LYP method in the commercially available Gaussian09). This results in somewhat higher barrier heights for CO_2 [1,3]-addition to PNN-Ru complex.

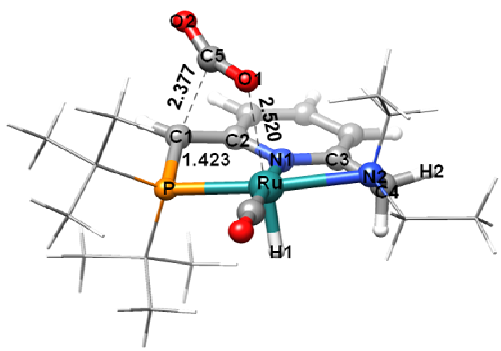

TS1/4

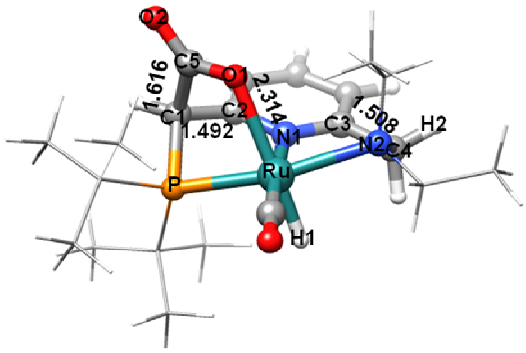

4

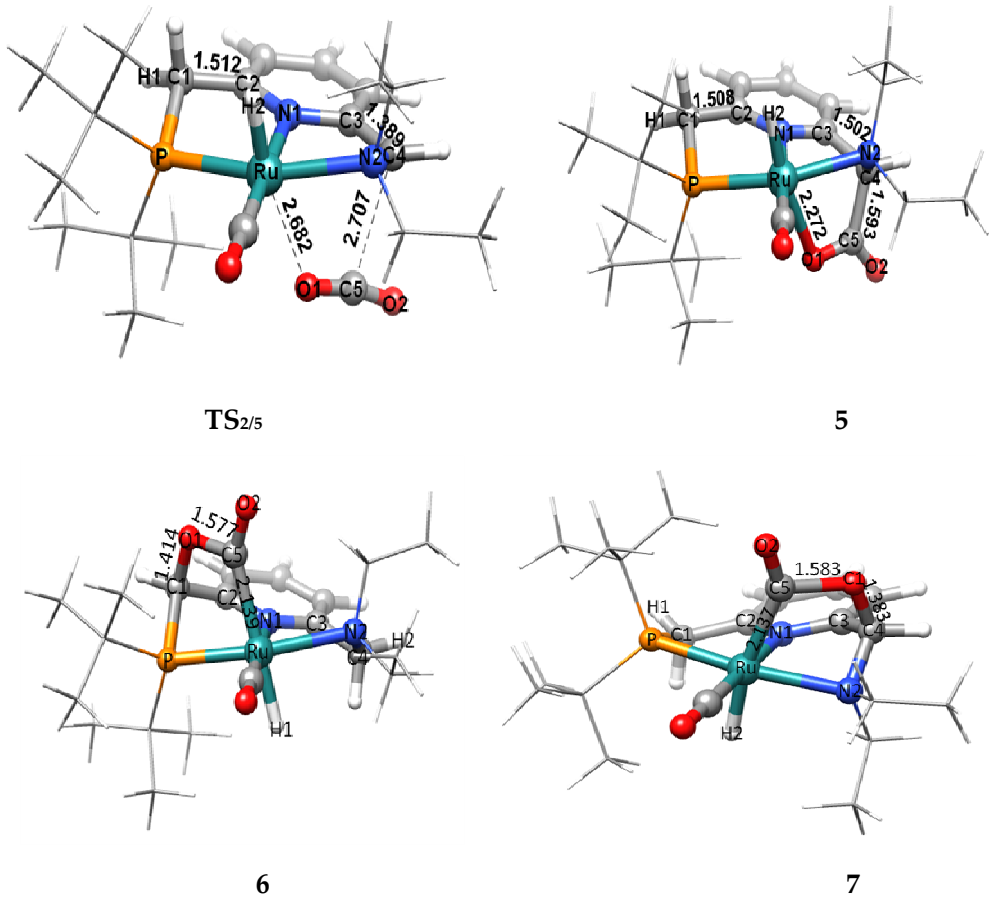

Figure 4: Optimized structures of the intermediates (**4**, **5, 6** and **7**) and the transition states (**TS**$_{1/4}$ and **TS**$_{2/5}$), along with the key bond lengths (Å).

4. Frontier Molecular Orbital analysis

For deeper understanding of the reaction mechanism, we performed Frontier Molecular Orbital (FMO) analysis for **1**, **2** and CO_2, and their highest occupied molecular orbital (HOMO) and lowest unoccupied molecular orbital (LUMO) are shown in **Figure 5**.

It can be seen that the energy difference between the HOMO of CO_2 and LUMO of **1** (0.32 hartree) is small while the energy difference between the LUMO of CO_2 and HOMO of **1** (0.45 hartree) is large. According to Frontier Molecular orbital theory, the main interaction between CO_2 and **1** occurs between the LUMO of **1** and the HOMO of CO_2, while the interaction between the LUMO of CO_2 and the HOMO of **1** plays a minor role. The HOMO

of CO_2 is composed of *p*-orbitals on the two O atoms, and the LUMO of **1** has large $5p_z$ and $4d_{z^2}$ components on Ru atom, this strongly favors O-Ru bond formation. The LUMO of CO_2 has a large *p*-orbital component on C atom and the HOMO of **1** has a large *p*-orbital component on the methylene C atom, this is conducive to the formation of C-C bond especially in the second half-reaction. In the reverse [1,3]-addition, shorten the distance between one O atom of CO_2 and the methylene C atom of **1** leads to strong repulsion between the HOMO of CO_2 and HOMO of **1**, therefore, reverse [1,3]-addition that leading to **6** is unfavorable.

Frontier Molecular Orbital analysis gives similar conclusion for CO_2 reaction with **2**. In addition, the relative stability of **4** and **5** can be elucidated by the overlapping efficiency of orbitals of the two reactants. The Ru-C1 distance in **1** is 3.19 Å, while Ru-C2 distance in **2** is 3.01 Å. The shorter Ru-C1 distance in **2** is beneficial to a stronger orbital interaction with O=C bond of CO_2, compared with the longer Ru-C2 distance in **1**. Therefore, CO_2 addition to **2** leads to a more stable product **5**.

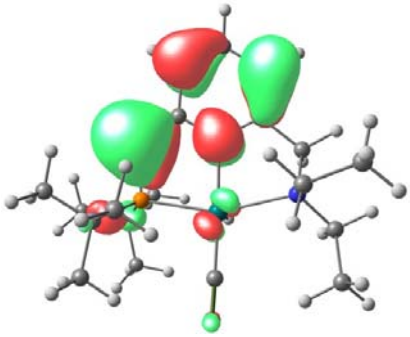

1-HOMO
(-0.15907)

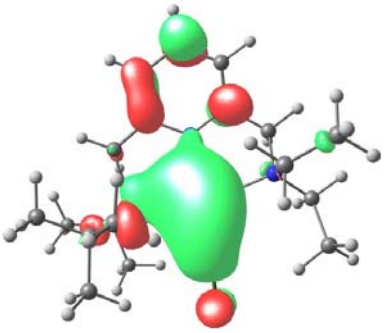

1-LUMO
(-0.05267)

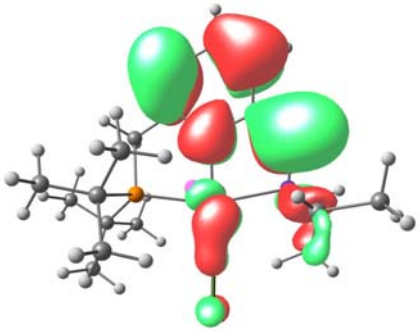

2-HOMO
(-0.14789)

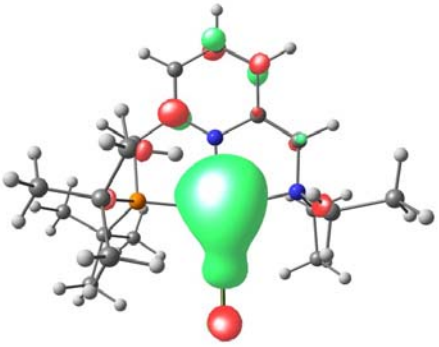

2-LUMO
(-0.04943)

CO_2-HOMO (-0.37686) CO_2-LUMO (0.2952)

Figure 5: The frontier molecular orbitals of **1**, **2** and CO_2. Orbital energies given in parenthesis (in hartree)

5. Conclusion

The reaction mechanism of CO_2 activation with unsaturated PNN-pincer complex (PNN)Ru(H)(CO) was investigated by B3LYP method, combined with IEFPCM solvation effect of C_6H_6 and dispersion correction by DFT-D3 model. Theoretical results show that: a) (PNN)Ru(H)(CO) isomer **1** (with the methylene in the phosphorus side arm) is more stable than **2** (with the methylene in the amide side arm) by 6.45 kcal/mol. Tautomerization of **1** and **2** involves nonhydride intermediate **3** and two hydrogen migration steps with barrier heights of 49.94 and 38.24 kcal/mol, respectively. b) The concerted [1,3]-addition of CO_2 to **1** and **2** involves C-C and Ru-O bond formation and leads to **4** and **5** with small barriers of 9.83 and 6.66 kcal/mol, respectively. **4** is less stable than **5** by 8.12 kcal/mol, and decomposition barriers for **4** and **5** are 7.97 and 19.38 kcal/mol, respectively. c) inverse [1,3]-addition of CO_2 to **1** and **2** leads to **6** and **7** is less competitive, since the **6** and **7** are located higher than the transition states of forming **4** and **5**, $\mathbf{TS_{1/4}}$ and $\mathbf{TS_{2/5}}$.

These results are in good agreement to the experimental facts. Frontier molecular orbital analysis confirmed that [1,3]-addition of CO_2 to **1** and **2** is symmetric allowed reaction, and C-C and O-Ru addition type (leading to **4** and **5**) is preferred to C-O and C-Ru addition type(leading to **6** and **7**). Shorter Ru-C(methylene) distance in **2** is beneficial to stronger overlap of the frontier molecular orbitals of **2** and CO_2, which leads to more stable product **5**.

Acknowledgments

The Project is supported by the Scientific Research Foundation for the Returned Overseas Chinese Scholars, Shanxi Province, P. R. China. Project No. 2008－75.

References

[1] J. Zhang, G. Leitus, Y. Ben-David, D. Milstein, Facile Conversion of Alcohols into Esters and Dihydrogen Catalyzed by New Ruthenium Complexes, J. Am. Chem. Soc., 127 (2005), 10840-10841.

[2] J. Zhang, M. Gandelman, L. J. W. Shimon, H. Rozenberg, D. Milstein, Electron-Rich, Bulky Ruthenium PNP-Type Complexes.Acceptorless Catalytic Alcohol Dehydrogenation, Organometallics, 23 (2004), 4026-4033.

[3] J. Zhang, M. Gandelman, L. J. Shimon, D. Milstein, Electron-rich, bulky PNN-type ruthenium complexes: synthesis, characterization and catalysis of alcohol dehydrogenation, Dalton transactions, 2007,107-113.

[4] M. Montag, J. Zhang, D. Milstein, Aldehyde binding through reversible C-C coupling with the pincer ligand upon alcohol dehydrogenation by a PNP-ruthenium catalyst, Journal of the American Chemical Society, 134 (2012), 10325-10328.

[5] M. Gargir, Y. Ben-David, G. Leitus, Y. Diskin-Posner, L. J. W. Shimon, D. Milstein, PNS-Type Ruthenium Pincer Complexes, Organometallics, 31 (2012), 6207-6214.

[6] J. Zhang, G. Leitus, Y. Ben-David, D. Milstein, Efficient homogeneous catalytic hydrogenation of esters to alcohols, Angewandte Chemie, 45 (2006), 1113-1115.

[7] E. Balaraman, B. Gnanaprakasam, L. J. W. Shimon, D. Milstein, N-H Activation of Amines and Ammonia by Ru via Metal-Ligand Cooperation, J. Am. Chem. Soc., 132 (2010), 16756-16758.

[8] E. Fogler, E. Balaraman, Y. Ben-David, G. Leitus, L. J. W. Shimon, D. Milstein, Electron-Rich PNP- and PNN-Type Ruthenium(II) Hydrido Borohydride Pincer Complexes. Synthesis, Structure, and Catalytic Dehydrogenation of Alcohols and Hydrogenation of Esters, Organometallics, 30 (2011), 3826-3833.

[9] E. Balaraman, Y. Ben-David, D. Milstein, Unprecedented catalytic hydrogenation of urea derivatives to amines and methanol, Angewandte Chemie, 50 (2011), 11702-11705.

[10] J. Zhang, E. Balaraman, G. Leitus, D. Milstein, Electron-Rich PNP- and PNN-Type Ruthenium(II) Hydrido Borohydride Pincer Complexes. Synthesis, Structure, and Catalytic Dehydrogenation of Alcohols and Hydrogenation of Esters, Organometallics, 30 (2011), 5716-5724.

[11] E. Balaraman, E. Fogler, D. Milstein, Efficient hydrogenation of biomass-derived cyclic di-esters to 1,2-diols, Chemical communications, 48 (2012), 1111-1113.

[12] Y. Chen, W. H. Fang., Mechanism for the Light-Induced O_2 Evolution from H_2O Promoted by Ru(II) PNN Complex: A DFT Study, J. Phys. Chem. A, 114 (2010), 10334-10338.

[13] G. Zeng, S. Li, Insights into dehydrogenative coupling of alcohols and amines catalyzed by a (PNN)-Ru(II) hydride complex: unusual metal-ligand cooperation, Inorganic chemistry, 50 (2011), 10572-10580.

[14] E. Khaskin, M. A. Iron., L. J. W. Shimon, J. Zhang, D. Milstein, N-H Activation of Amines and

Ammonia by Ru via Metal-Ligand Cooperation, J. Am. Chem. Soc., 132 (2010), 8542-8543.

[15] X. Yang, Metal Hydride and Ligand Proton Transfer Mechanism for the Hydrogenation of Dimethyl Carbonate to Methanol Catalyzed by a Pincer Ruthenium Complex, ACS Catalysis, 2 (2012), 964-970.

[16] H. Li, X. Wang, F. Huang, G. Lu, J. Jiang, Z.-X. Wang, Computational Study on the Catalytic Role of Pincer Ruthenium(II)-PNN Complex in Directly Synthesizing Amide from Alcohol and Amine: The Origin of Selectivity of Amide over Ester and Imine, Organometallics, 30 (2011), 5233-5247.

[17] M. Vogt, M. Gargir, M. A. Iron, Y. Diskin-Posner, Y. Ben-David, D. Milstein, A New Mode of Activation of CO_2 by Metal–Ligand Cooperation with Reversible C-C and M-O Bond Formation at Ambient Temperature, Chem. Eur. J., 18 (2012), 9194 – 9197.

[18] C. A. Huff, J. W. Kampf, M. S. Sanford , Role of a Noninnocent Pincer Ligand in the Activation of CO_2 at (PNN)Ru(H)(CO), Organometallics, 31 (2012), 4643-4645.

[19] P. G. Jessop, F. Joó, C.-C. Tai, Recent advances in the homogeneous hydrogenation of carbon dioxide, Coordination Chemistry Reviews, 248 (2004), 2425-2442.

[20] M. J. Frisch, et al. Gaussian03, revision E.01; Gaussian, Inc.: Wallingford, CT, 2004.

[21] C. Gonzalez, H. B. Schlegel, An improved algorithm for reaction path following, J. Chem. Phys., 90 (1989), 2154-2161.

[22] M. J. Frisch, et al. Gaussian09, revision A.01; Gaussian, Inc.: Wallingford, CT, 2009.

[23] B. Mennucci, J. Tomasi, Continuum solvation models: A new approach to the problem of solute's charge distribution and cavity boundaries, J. Chem. Phys., 106 (1997), 5151-5158.

[24] E. Cancès, B. Mennucci, J. Tomasi, A new integral equation formalism for the polarizable continuum model: Theoretical background and applications to isotropic and anisotropic dielectrics, J. Chem. Phys., 107 (1997), 3032-3041.

[25] M. Cossi, V. Barone, B. Mennucci, J. Tomasi, Ab initio study of ionic solutions by a polarizable continuum dielectric model, Chem. Phys. Lett., 286 (1998), 253-260.

[26] M. Cossi, G. Scalmani, N. Rega, V. Barone, New developments in the polarizable continuum model for quantum mechanical and classical calculations on molecules in solution, J. Chem. Phys., 117 (2002), 43-54.

[27] B. Mennucci, E. Cancès, J. Tomasi, Evaluation of Solvent Effects in Isotropic and Anisotropic Dielectrics and in Ionic Solutions with a Unified Integral Equation Method: Theoretical Bases, Computational Implementation, and Numerical Applications, J. Phys. Chem. B, 101 (1997), 10506-10517.

[28] J. Tomasi, B. Mennucci, E. Cancès, J. Mol. Struct. (THEOCHEM), The IEF version of the PCM solvation method: an overview of a new method addressed to study molecular solutes at the QM ab initio level, 464 (1999), 211-226.

[29] A. V. Marenich, C. J. Cramer, D. G. Truhlar, Universal Solvation Model Based on Solute Electron Density and on a Continuum Model of the Solvent Defined by the Bulk Dielectric Constant and

Atomic Surface Tensions, J. Phys. Chem. B, 113 (2009), 6378-6396.

[30] T. Schwabe, S. Grimme, Double-hybrid density functionals with long-range dispersion corrections: higher accuracy and extended applicability, Phys. Chem. Chem. Phys., 9 (2007), 3397-3406.

[31] S. Grimme, J. Antony, S. Ehrlich, H. Kreig, A consistent and accurate ab initio parametrization of density functional dispersion correction (DFT-D) for the 94 elements H-Pu, J. Chem. Phys., 132 (2010), 154104.

[32] http://toc.uni-muenster.de/DFTD3/, accessed July 13, 2010.